Preparation and Electrical Properties of Highly (111)-Oriented $(Na_{0.5}Bi_{0.5})TiO_3$ Thin Films by a Sol−Gel Process

Xin-Gui Tang,* Jie Wang, Xiao-Xing Wang, and Helen Lai-Wah Chan

Department of Applied Physics and Materials Research Centre, The Hong Kong Polytechnic University, Hung Hom, Kowloon, Hong Kong, China

Received November 26, 2003. Revised Manuscript Received July 15, 2004

Sodium bismuth titanate, $(Na_{0.5}Bi_{0.5})TiO_3$ (NBT), thin films were grown on Pt/Ti/SiO_2/Si substrates via a sol−gel process. The precursor solution for spin-coating was prepared from bismuth nitrate, sodium acetate, and titanium *n*-butoxide as starting materials, and acetic acid and methanol as solvents, and pervoskite NBT films with high (111)-orientation have been obtained. The Au/NBT/Pt thin film capacitor showed a hysteresis loop at an applied electric field of 200 kV/cm with remanent polarization (P_r) and coercive electric field (E_c) values of 20.9 μC/cm^2 and 112 kV/cm, respectively. At 100 kHz, the dielectric constant and loss tan δ of the film were 171 and 0.024, respectively. The leakage current depended on the voltage polarity. When an electrical field ranges from 0 to 167 kV/cm and with the Pt electrode biased negatively, the NBT/Pt interface exhibits a Schottky emission characteristic. The Au/NBT interface forms an ohmic contact. The conduction current when the Au electrode is biased negatively shows space-charge-limited current (SCLC) behavior.

Introduction

Sodium bismuth titanate, $(Na_{0.5}Bi_{0.5})TiO_3$, is an A-site complex perovskite relaxor ferroelectric discovered by Smolenskii et al.[1] In recent years, $(Na_{0.5}Bi_{0.5})TiO_3$ and $(Na_{0.5}Bi_{0.5})TiO_3$-based materials are lead-free ferroelectric materials, which attracted considerable research attention due to their excellent piezoelectric properties and unclear phase behavior.[2−14] The highest temperature phase of $(Na_{0.5}Bi_{0.5})TiO_3$ is cubic, and it undergoes a phase transition to tetragonal at 540−530 °C, and to rhombohedral at about 200 °C.[15] The tetragonal and rhombohedral phases are known to exhibit ferroelasticity and ferroelectricity, respectively. A broad maximum of relative permittivity occurs at about 320 °C, which manifests the phase transition. The phase transition to the ferroelectric state at about 200 °C appears as a small broad anomaly in the dielectric constant with a weak relaxor behavior. The sol−gel-derived pure $(Na_{0.5}Bi_{0.5})TiO_3$ ceramics have good ferroelectric (P_r = 32 μC/cm^2 and E_c = 61 kV/cm) and piezoelectric properties (d_{33} = 102 pC/N and k_p = 56%).[16] In our previous work, we have prepared excess Bi_2O_3- and CeO_2-doped $(Na_{0.5}Bi_{0.5})TiO_3$-based ceramics.[17,18] At room temperature, the sample containing 0.4 wt % CeO_2 shows good ferroelectric properties (P_r = 37.7 μC/cm^2, E_c = 37.1 kV/cm) with a high piezoelectric constant (d_{33} = 152 pC/N) and coupling factor (k_p = 34%). However, there is no literature reported on the preparation and electrical properties of $(Na_{0.5}Bi_{0.5})TiO_3$ films; $(K_{0.5}Bi_{0.5})TiO_3$ films that have slightly ferroelectric properties have been reported.[19]

In this work, $(Na_{0.5}Bi_{0.5})TiO_3$ thin films were synthesized via a sol−gel process. The aim of this work is to examine the structural, ferroelectric, dielectric, and leakage current characteristics of $(Na_{0.5}Bi_{0.5})TiO_3$ thin films.

Experimental Section

$(Na_{0.5}Bi_{0.5})TiO_3$ (abbreviated as NBT) thin films were prepared via a sol−gel technique with spinning-on process.[16,20] Weighted amounts of appropriate proportions of high-purity bismuth nitrate $Bi(NO_3)_3{\cdot}5H_2O$, sodium acetate $Na(CH_3COO)$,

* Corresponding author. Fax: +852-2333 7629. E-mail: xgtang6@yahoo.com.

(1) Smolenskii, G. A.; Isupov, V. A.; Agranovskaya, A. I.; Kainik, N. N. *Sov. Phys. Solid State* **1961**, *2*, 2651.
(2) Jones, G. O.; Thomas, P. A. *Acta Crystallogr., Sect. B* **2000**, *56*, 426.
(3) Jones, G. O.; Thomas, P. A. *Acta Crystallogr., Sect. B* **2002**, *58*, 168.
(4) Jaffe, B.; Cook, W. R., Jr.; Jaffe, H. *Piezoelectric Ceramics*; Academic Press: New York, 1971; pp 205−206.
(5) Chiang, Y.; Farrey, G. W.; Soukhojak, A. N. *Appl. Phys. Lett.* **1998**, *73*, 3683.
(6) Kuharuanhrong, S.; Schulze, W. *J. Am. Ceram. Soc.* **1997**, *78*, 2274.
(7) Isupov, V. S.; Strelets, P. L.; Scrova, I. A. *Sov. Phys. Solid State* **1964**, *6*, 615.
(8) Sakata, K.; Masuda, Y. *Ferroelectrics* **1974**, *7*, 347.
(9) Park, S. E.; Hong, K. S. *J. Appl. Phys.* **1996**, *79*, 388.
(10) Herabut, A.; Safari, A. *J. Am. Ceram. Soc.* **1997**, *80*, 2954.
(11) Roleder, K.; Franke, I.; Glazer, A. M.; Thomas, P. A.; Miga, S.; Suchanicz, J. *J. Phys.: Condens. Matter* **2002**, *14*, 5399.
(12) Suchanicz, J.; Mercurio, I. P.; Marchet, P.; Kruzina, T. V. *Phys. Status Solidi B* **2001**, *225*, 459.
(13) Kreisel, J.; Glazer, A. M.; Bouvier, P.; Lucazeau, G. *Phys. Rev. B* **2001**, *63*, 174106.
(14) Chu, B. J.; Chen, D. R.; Li, G. R.; Yin, Q. R. *J. Eur. Ceram. Soc.* **2002**, *22*, 2115.
(15) Kusz, J.; Suchanicz, J.; Bohm, H.; Warczewski, J. *Phase Transitions* **1999**, *70*, 223.
(16) Zhao, M. L.; Wang, C. L.; Zhong, W. L.; Wang, J. F.; Chen, H. C. *Acta Phys. Sin.* **2003**, *52*, 229. Zhao, M. L.; Wang, C. L.; Zhong, W. L.; Wang, J. F.; Li, Z. F. *Chin. Phys. Lett.* **2003**, *20*, 290.
(17) Wang, X. X.; Chan, H. L. W.; Choy, C. L. *Solid State Commun.* **2003**, *125*, 395.
(18) Wang, X. X.; Tang, X. G.; Kwok, K. W.; Chan, H. L. W.; Choy, C. L. *Appl. Phys. A* **2004**, *79*, in press.
(19) Li, Z. F.; Wang, C. L.; Zhong, W. L.; Li, J. C.; Zhao, M. L. *J. Appl. Phys.* **2003**, *94*, 2548.

10.1021/cm035222l CCC: $27.50
Published on Web 11/12/2004

and titanium *n*-butoxide $Ti(OC_4H_9)_4$ were used as precursors. Acetic acid CH_3COOH and methanol CH_3OH were selected as solvents, and acetylacetone ($C_5H_8O_2$) was selected as a reagent to stabilize titanium *n*-butoxide. Bismuth nitrate and sodium acetate were dissolved in acetic acid, with stirring for 120 min at 70 °C. Titanium *n*-butoxide was dissolved in methanol, with stirring for 60 min at 70 °C, and the appropriate proportions of acetylacetone were added to stabilize the titanium *n*-butoxide solution. After being cooled to room temperature, the two solutions were mixed in a flask at 70 °C. The complex Bi−Na−Ti solution was then stirred for 60 min, without using reflux and high-temperature distillation to remove water. The precursor with 10% excess Bi composition was prepared on purpose to compensate for the bismuth loss in the deposition processing. The concentration of the final solution can be adjusted to 0.3 M and a pH value of 2−4 by adding acetic acid and methanol. The whole process of the preparation of the precursor solution is performed in an ambient atmosphere.

Before spin-coating on the Pt(111)/Ti/SiO_2/Si(100) substrates, the solution was filtered with a porous site of the filter paper to avoid particulate contamination. The thermal treatment process for the samples was completed with a hot plate and a rapid thermal annealing (RTA) furnace. The NBT coating solution was deposited onto Pt/Ti/SiO_2/Si substrates by spin-coating at 3600 rpm for 30 s. After each spin-coating process, the samples were heat-treated on a hot plate at 300 °C for 10 min in an air atmosphere. This step was repeated four times to obtain the desired thickness of the films. The NBT films on Pt/Ti/SiO_2/Si substrates were annealed at 600−650 °C for 10 min by RTA in an oxygen atmosphere. The heating rate was 100 °C/s. The thickness of the NBT films on Pt/Ti/SiO_2/Si substrates, as measured by a spectroscopic ellipsometer (ISA Obin-Yvon, UVISEL/460, France), was 300 nm.

Structures of the NBT thin films on Pt/Ti/SiO_2/Si substrates were analyzed by a Philips Expert System X-ray diffractometer. The surface morphology of the films was characterized by a NanoScope IIIa (Digital, USA) atomic force microscope (AFM). The composition of NBT films was determined by Rutherford backscattering spectroscopy (RBS) and ion channeling. To investigate the electrical properties of the NBT thin films, top gold (Au) electrodes of 0.4 mm diameter were prepared on the top surface of the NBT films through a shadow mask in a vacuum by rf-magnetron sputtering. The polarization−electric-field (*P*−*E*) hysteresis loop was obtained using a TF Analyzer 2000 (aix-ACCT, Aachen, Germany) system with a 100 Hz sinusoidal input signal. The dielectric properties of the NBT films were measured by an HP4292A impedance analyzer with a small ac signal of 500 mV. The leakage current (*I*−*V*) characteristics measurement was carried out with a Keithley 6517A programmable electrometer. Staircase-shaped dc bias voltages, with a 0.1 V step and 3 s span, were applied to the top electrodes, while the bottom electrodes were grounded. Several preliminary measurements confirmed that the *I*−*V* measurement procedure was good enough to obtain steady-state leakage currents.

Results and Discussion

Figure 1 shows the X-ray diffraction (XRD) pattern of NBT thin films on Pt/Ti/SiO_2/Si substrates annealed at 600 and 650 °C for 10 min in an oxygen atmosphere by RTA. In the film annealed at 600 °C, a broad diffraction peak was observed near 29°; they are second phases.[6] As the annealing temperature was increased to 650 °C, the film was completely crystallized to the perovskite NBT phase.[1−3,21] The XRD results also exhibit that the crystalline NBT films, annealed at 600 °C, displayed very strong (111) orientation. When the

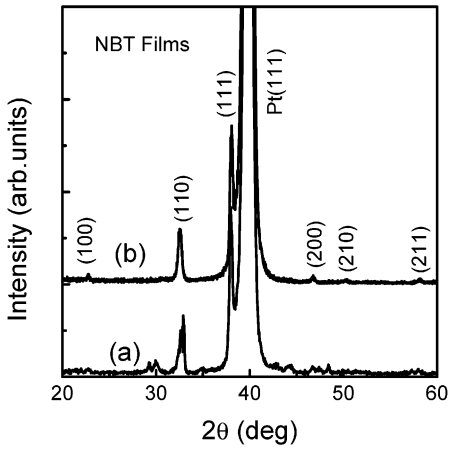

Figure 1. XRD patterns of NBT films on Pt/Ti/SiO_2/Si substrates. The film has been annealed at (a) 600 and (b) 650 °C for 10 min in oxygen atmosphere by RTA.

NBT film was annealed at 650 °C for 10 min, a single phase of perovskite structure with rhombohedral symmetry was observed. The degree of the (111)-type preferential growth, as estimated using the Lotgering factor,[22] is 71.5%. Tani et al.[23] suggested that whenever the Ti from the adhesion layer formed (111) Pt_3Ti on the surface, a (111) perovskite PLZT texture was obtained. The preferred (111) orientations are due to the coexistence of Ti at the interface Pt and PLZT. In this Pt_3Ti cubic structure, the *d* spacing of Pt_3Ti was 2.254 Å. In the structure of the rhombohedral phase of the A-site-substituted perovskite NBT films, the *d* spacing was 2.351 Å (from XRD). The lattice-mismatch was less than 4.2%. Thus, the nuclei have a preferred (111) orientation because of the Pt_3Ti acting as a lattice-matching buffer layer between the Pt and NBT. When the film has this perovskite seeding layer, the activation energy for the crystallization of the films decreases. If the film is then subjected to a higher temperature heat treatment, the (111) nuclei will grow and strong (111) texture develops in accordance with the minimum surface energy conditions.

Figure 2 shows the AFM image of NBT thin film on Pt/Ti/SiO_2/Si substrate annealed at 650 °C for 10 min in an oxygen atmosphere by RTA. It is seen from the surface image of NBT thin film that the grain size ranges from 0.2 to 1.5 μm. Many clusters exhibit in the surface, which are composed of nanosized grains with a size of about 200 nm. The root-mean-square (RMS) roughness of the film surfaces is 7.3 nm.

The experimental and simulated RBS spectrum of the NBT film on Pt/Ti/SiO_2/Si substrate was given in Figure 3. In the measurements, a 2 MeV He^+ ion beam from a 2 MV tandem accelerator was used at The Chinese University of Hong Kong. The ion beam size was 1 mm in diameter with a divergence of 0.05°. A surface barrier detector with a resolution of 17 keV was used at a scattering angle of 170°. The energy of the ions backscattered at the surface of Na, Bi, and Ti appears at 470, 895, and 690 channel numbers, which are labeled in Figure 3. As expected, the obtained NBT films have a composition of $(Na_{0.5}Bi_{0.5})TiO_3$.

(20) Tang, X. G.; Ding, A. L.; Ye, Y.; Chen, H. L. W. *Chem. Mater.* **2002**, *14*, 2129.
(21) Nagata, H.; Takenaka, T. *J. Eur. Ceram. Soc.* **2001**, *21*, 1299.
(22) Lotgering, F. K. *J. Inorg. Nucl. Chem.* **1959**, *9*, 113.
(23) Tani, T.; Xu, Z.; Payne, D. A. *Mater. Res. Soc. Symp. Proc.* **1993**, *310*, 269.

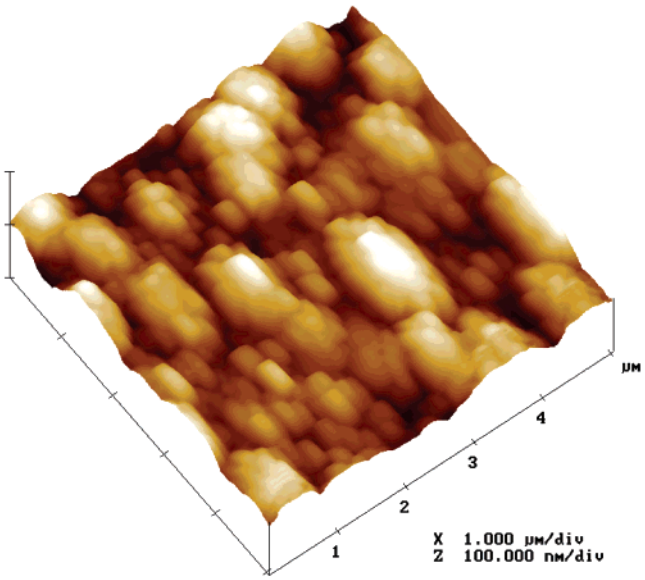

Figure 2. AFM image for NBT film on Pt/Ti/SiO_2/Si substrate. The film has been annealed at 650 °C for 10 min in an oxygen atmosphere by RTA. Area: 5×5 μm^2.

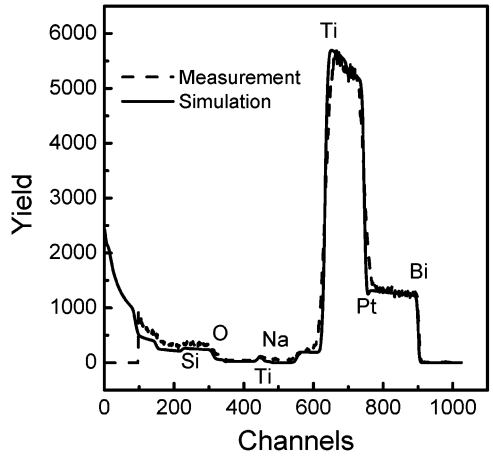

Figure 3. RBS spectrum of the NBT thin film on Pt/Ti/SiO_2/Si substrate. The film has been annealed at 650 °C for 10 min in oxygen atmosphere by RTA (- - -, experimental; −, theoretical).

Figure 4 shows a typical polarization−electric field (P−E) hysteresis loop for the NBT films on Pt/Ti/SiO_2/Si substrates annealed at 650 °C. The spontaneous polarization (P_s), remanent polarization (P_r), and the coercive electric field (E_c) obtained from the P−E hysteresis loops are 29.8 μC/cm^2, 20.9 μC/cm^2, and 112 kV/cm, respectively. The remanent polarization is lower, while the coercive field is higher, than that of sol−gel-derived bulk NBT ceramics (32 μC/cm^2, 61 kV/cm)[16] and is lower, while the coercive field is higher, than that of spark-plasma-sintering derived bulk NBT-BT ceramics (37.7 μC/cm^2, 37.1 kV/cm).[17] $Ki_{0.5}Bi_{0.5}TiO_3$ films have slightly ferroelectric properties.[19] The ferroelectric critical size of NBT bulk materials was about 100 nm.[16] The NBT thin films have large cluster grain sizes (see Figure 2), so that the ferroelectric properties in NBT thin films are partly from the existence of large cluster grains. On the other hand, large leakage currents exist in the films. In this case, the leakage currents also partly contribute to the ferroelectric behavior.

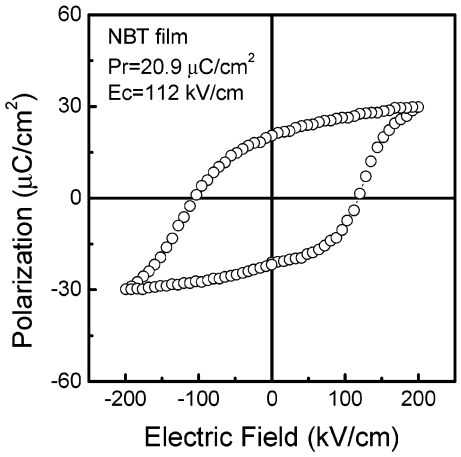

Figure 4. Typical P−E hysteresis loop for the NBT thin film on Pt/Ti/SiO_2/Si substrate. The film has been annealed at 650 °C for 10 min in oxygen atmosphere by RTA.

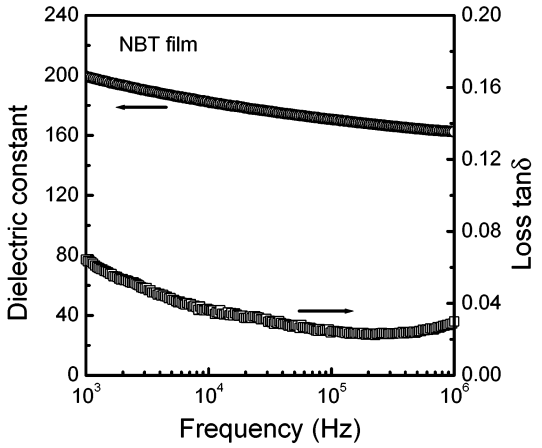

Figure 5. Dielectric constant and loss tan δ as a function of frequency for the NBT film. The film has been annealed at 650 °C for 10 min in oxygen atmosphere by RTA.

Figure 5 shows the variation of dielectric constant and loss tan δ as a function of frequency for the NBT films. The dielectric constants and loss tan δ change from 196 to 162 and from 0.064 to 0.030 with increasing frequency from 1 kHz to 1 MHz, respectively. At 100 kHz, the dielectric constant and loss tan δ were 171 and 0.024, respectively.

Figure 6 shows the current density as a function of voltage when the Pt electrode is negatively and positively biased in the voltage range of −5 to 5 V. The leakage current density was lower than 4.5×10^{-5} A/cm^2 over the voltage range of 0 to ±5 V. When the dc bias was lower than 4.3 V, the leakage current with the Pt electrode under a positive bias voltage was slightly lower than when the Pt electrode was under a negative voltage. In fact, the leakage currents in two opposite directions were limited by the interfaces between the film and Pt or Au electrodes,[24−26] respectively. The positive leakage current was limited by the interface between the Pt bottom electrode and the NBT thin film (the bottom interface), while the negative leakage

(24) Zafar, S.; Jones, R. E.; Jiang, B.; White, B.; Kaushik, V.; Gillespie, S. *Appl. Phys. Lett.* **1998**, *73*, 3533.
(25) Dietz, G. W.; Schumacher, M.; Waser, R.; Streiffer, S. K.; Basceri, C.; Kingon, A. I. *J. Appl. Phys.* **1999**, *82*, 2359.
(26) Tang, X. G.; Wang, J.; Zhang, Y. W.; Chan, H. L. W. *J. Appl. Phys.* **2003**, *94*, 5163.

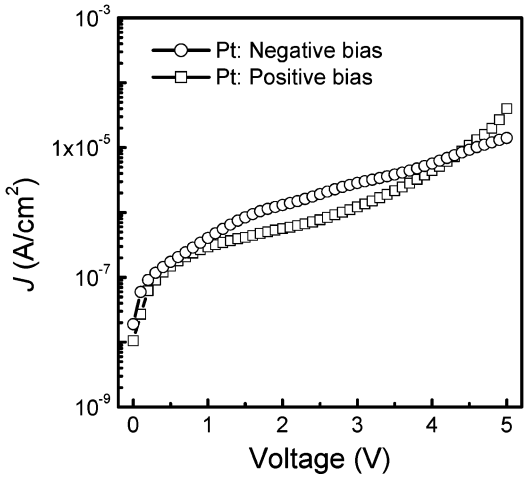

Figure 6. Leakage current density versus dc bias voltage characteristics for the Au/NBT/Pt thin film capacitor.

current was limited by the interface between the Au top electrode and the NBT film (the top interface). Therefore, the electrical quality is slightly better at the top interface than at the bottom interface at low voltage (4.3 V).

The leakage current depends on the bias polarity. As a result, the conduction mechanism should be electrode limited for at least one of the metal−insulator junctions. Although the origin of the observed leakage current is not known, several mechanisms, including Schottky emission,[27−29] Frenkel−Poole emission,[30] and space-charge-limited current (SCLC),[31] may simultaneously contribute to the leakage current with one of them playing the main role. The Schottky emission can be expressed as log J (where J is the leakage current density), proportional to the square root of the applied electrical field (E). The space-charge-limited current (SCLC) can be expressed as log J, proportional to log E.

To verify the Schottky-dominated conduction in NBT thin films, the current density J was plotted against $E^{1/2}$ in the semilog scale, which was supposed to be a straight line. The Schottky plot for NBT thin films is shown in Figure 7a, where linearity was observed. The leakage current shows a Schottky emission behavior when the Pt electrode was under a negative bias voltage. The NBT/Pt interface forms a Schottky barrier at the dc bias range from 0 to 5 V. The Schottky emission mechanism is an electrode-limited conduction, where the entire leakage current is dominated by the Schottky barrier generated at the interface of the electrode and films. Figure 7b shows the plot of log(J) versus log(E) with the Au electrode biased when there is a negative voltage for the Au/NBT/Pt thin film capacitors. The slope is close to 1.0 in the low electric field (100 kV/cm) region. The Au/NBT contact is thus ohmic in the low electric field. At low field (100 kV/cm), the J−E characteristics followed Ohm's law because the density of thermally

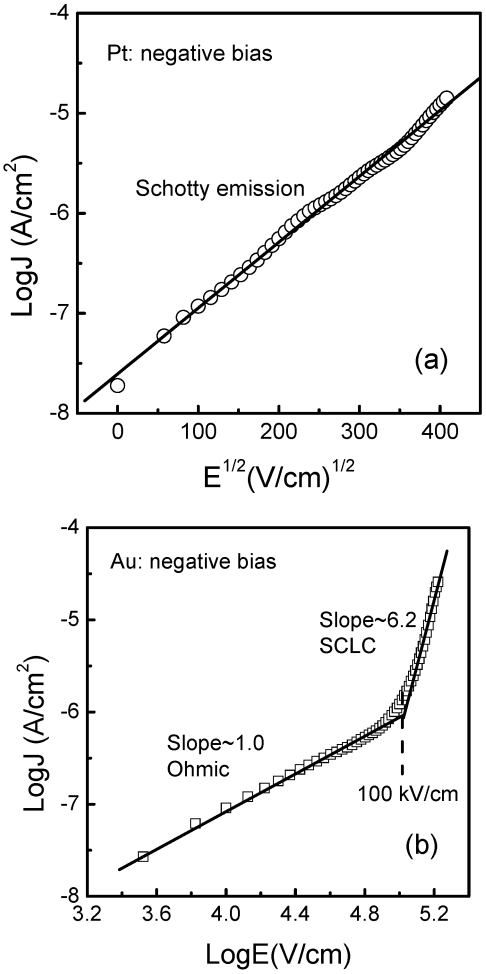

Figure 7. (a) Plot of log(J) versus $(E)^{1/2}$ when the Pt electrode of the Au/NBT/Pt thin film capacitor was under a negative bias. (b) Plot of log(J) versus log(E) when the Au electrode of the Au/NBT/Pt thin film capacitor was under a negative bias.

generated carriers in the films was predominant over the injected charge carriers. At a field above 100 kV/cm, the plot of log(J) versus log(E) shows a slope that is close to 6.2, which agrees well with SCLC theory.[31]

Conclusions

In summary, NBT films were grown on Pt/Ti/SiO_2/Si substrates by a sol−gel process with a rapid thermal annealing process. The NBT film annealed at 650 °C for 10 min has a grain size of about 200 nm. The highly (111)-oriented NBT film has a remanent polarization and coercive electric field of 20.9 μC/cm^2 and 112 kV/cm. The leakage current depended on the voltage polarity. At low electrical field and with the Pt electrode biased negatively, the NBT/Pt interface exhibits a Schottky emission characteristic. At low field (<100 kV/cm), the Au/NBT interface forms an ohmic contact, while at high field (>100 kV/cm), the conduction current when the Au electrode is biased negatively shows space-charge-limited current behavior.

Acknowledgment. This work was supported by the Postdoctoral Fellowship Scheme and the Center for Smart Materials of the Hong Kong Polytechnic University.

CM035222L

(27) Scott, J. F.; Melnick, B. M.; Araujo, C. A.; Mcmillan, L. D.; Zuleez, R. *Integr. Ferroelectr*. **1992**, *1*, 323.
(28) Zafar, S.; Jones, R. E.; Jiang, B.; White, B.; Kaushik, V.; Gillespie, S. *Appl. Phys. Lett*. **1991**, *70*, 382.
(29) Watanabe, K.; Hartmann, A. J.; Lamb, R. N.; Scott, J. F. *J. Appl. Phys*. **1998**, *84*, 2170.
(30) Wang, Y.; Tseng, T. Y. *J. Appl. Phys*. **1997**, *81*, 6762.
(31) Scott, J. F. *Ferroelectric Memories*; Springer: Berlin, 2000.